Available online at www.sciencedirect.com
ScienceDirect
Bioelectrochemistry 70 (2007) 542–550
Bioelectrochemistry
www.elsevier.com/locate/bioelechem

Protein influence on the plasma membrane dielectric properties: In vivo study utilizing dielectric spectroscopy and fluorescence microscopy

M. Stoneman [a], A. Chaturvedi [a], D.B. Jansma [a], M. Kosempa [a], C. Zeng [b], V. Raicu [a,b,*]

[a] Department of Physics, University of Wisconsin-Milwaukee, PO Box 413, Milwaukee, WI 53201, USA
[b] Department of Biological Sciences, University of Wisconsin-Milwaukee, PO Box 413, Milwaukee, WI 53201, USA

Received 25 October 2006; received in revised form 11 December 2006; accepted 28 December 2006
Available online 13 February 2007

Abstract

We have investigated the origin of the dielectric response of the plasma membrane of *living* yeast cells (*Saccharomyces cerevisiae*) by using radiofrequency dielectric spectroscopy. The cells were genetically engineered to overexpress in the membrane of yeast cells a G protein-coupled receptor – the Sterile2-α factor receptor protein (Ste2p) – fused to the green fluorescent protein (GFP). Presence of the Ste2-GFP proteins in the plasma membrane was confirmed by exciting the cells at 476 nm and observing with a confocal microscope the emission characteristic of the GFP from individual cells. The dielectric behavior of cells suspended in KCl solution was analyzed over the frequency range 40 Hz–110 MHz and compared to the behavior of control cells that lacked the ability to express Ste2p. A two-shell electrical cell model was used to fit the data starting from known structural parameters and adjustable electrical phase parameters. The best-fit value for the relative permittivity of the plasma membrane showed no significant difference between cells expressing Ste2p (1.63±0.11) and the control cells (1.75±0.16). This result confirmed earlier predictions that the dielectric properties of the plasma membrane in the radiofrequency range mostly reflect the properties of the hydrophobic layer of the membrane, which is populated by the hydrocarbon tails of the phospholipids and hydrophobic segments of integral membrane proteins. We discuss ways by which dielectric spectroscopy can be improved to be used for *tag-free detection* of proteins on the membrane.

Keywords: Permittivity; Conductivity; Yeast; Cell suspension; Tag-free detection; Fluorescence

1. Introduction

Dielectric spectroscopy has been used as a technique to probe biological systems since the early twentieth century, but large-scale studies with high accuracy have been only facilitated by the advent of fast impedance analyzers in late 1980s. As early as 1925, at a time when microscopy techniques were not developed sufficiently to study the plasma membrane, Fricke determined its thickness using dielectric measurements of red blood cells [1,2]. Ensuing studies using dielectric spectroscopy have reported on the structures of numerous types of cell suspensions and tissues, and also time-dependent processes involving them, such as cell sedimentation [3], cell aggregation [4], cell division [5], and tissue viability after excision [6].

The underlying principles of dielectric spectroscopy are rather simple. When a direct current is applied to a dielectrically inhomogeneous material, charge is built up at the interfaces between different dielectric phases, causing the equivalent dielectric constant of the whole material to increase. If the applied current is alternating with variable frequency, the accumulation of charge will transiently follow the change in polarity of the applied current, and will eventually lose the pace at high enough frequencies; this leads to frequency dependence (or dispersion) of the permittivity, causing the permittivity to decrease at high frequencies. On the other hand, losses in the system follow an opposite tendency, leading to an increase in conductivity (or the inverse of resistivity) as the frequency increases.

Three major dispersions have been defined in the literature, each characterized by a different frequency range and due to a

* Corresponding author. Department of Physics, University of Wisconsin-Milwaukee, PO Box 413, Milwaukee, WI 53201, USA. Tel.: +1 414 229 4969; fax: +1 414 229 5589.
E-mail address: vraicu@uwm.edu (V. Raicu).

1567-5394/$ - see front matter © 2007 Elsevier B.V. All rights reserved.
doi:10.1016/j.bioelechem.2006.12.008

specific mechanism. Alpha dispersion occurs at low frequencies (~100 Hz) and is due to the presence of counterions [7]. Gamma dispersion, which occurs at ultrahigh frequencies (10 GHz), is attributed to the relaxation of water. The final major dispersion is termed the Beta dispersion, which occurs at radiofrequencies and is due the effect of interfacial polarization of cellular membranes, such as the plasma membrane. By analyzing the beta dispersion, one can determine the dielectric properties of the plasma membrane and of organellar membranes, as well as the properties of intracellular fluids, such as the cytosol.

Fluorescence imaging is a widespread and well developed biological tool of investigation, which provides useful information in many areas of research [8–13]. One specific area of great importance is the study of protein localization, activity, and interactions in living cells by using fluorescent tags attached to the protein of interest. The gene responsible for expression of a protein of interest can be fused to the gene of a naturally fluorescing protein, such as the green fluorescent protein (GFP), so that the host cell synthesizes the protein of interest with fluorescent tags attached to it. By optically exciting individual cells containing these proteins in a microscope or a suspension of cells in a spectrofluorometer, one detects emission of light characteristic of the fluorescent molecules fused to the proteins. In this manner, the localization of proteins in the cell can be verified and quantified to varying degrees.

Despite their widespread use and incontestable usefulness, fluorescence microscopy techniques require tagging, which may perturb the activity of the protein under study. On the other hand, it has been proposed recently [14,15] that detection of linear and nonlinear dielectric properties of the cell may eventually lead to noninvasive methods for detection of receptor proteins on the plasma membrane and for monitoring their activity and interactions in vivo, without recourse to tagging. This program is very appealing and deserves careful consideration. To this end, it is very important to investigate possible strengths and also challenges that need to be addressed before viable methods and theoretical models can be developed that directly relate protein localization and activity to measurable dielectric parameters. An important avenue of research in this area is investigation of the connection between the dielectric properties of the proteins and the overall properties of the cell suspension, the cell, or the different cell compartments (such as plasma membrane).

The goals of this paper are (a) to investigate the contributions of the main molecular components of the membrane to the measured membrane permittivity, and (b) to contribute to the experimental and theoretical foundations of the above research program by using linear dielectric spectroscopy in the audio/radiofrequency range to detect the presence of receptor proteins in the plasma membrane of the yeast *Saccharomyces cerevisiae*. Using DNA manipulation techniques, yeast cells were prepared expressing Ste2 receptor proteins — a widely investigated receptor that belongs to the G protein-coupled receptor family of proteins and is responsible for the signaling response that leads to mating in yeast cells [16–18]. The gene encoding Ste2p was inserted into a plasmid with a high copy number (typically, 50–200 copies per cell, each able to generate hundreds of receptor molecules in the cell). Therefore, high amounts of proteins were expressed in the cells. Ste2 receptors were tagged with green fluorescent protein (GFP), allowing their presence on the membrane of the cells to be confirmed by laser scanning confocal microscopy. Also prepared was a "control" sample with all of the properties found in the previously described strain, except for the presence of Ste2p. Comparisons between the dielectric properties, specifically the parameter describing the complex permittivity of the plasma membrane, of the cells expressing Ste2p and the control cells lacking Ste2p were performed to clarify the contribution of the proteins to the plasma membrane dielectric properties.

2. Theory

Dielectric properties of cell suspensions in the radiofrequency range are dominated by interfacial polarization, i.e., the accumulation of charge at the interface between conducting and insulating layers of the cell and its internal organelles [19,20]. Conducting compartments are, for example, the outer medium and the cytoplasm, which are rich in electrolyte, while insulating layers are represented by the membranes of the cell (plasma membrane) and its organelles. Various electrical models have been developed to describe different structural features of the cells, which are generally referred to in terms of shells (i.e., membranes). Yeast cells covered with a plasma membrane and possessing a vacuole have been described by the spherical or spheroidal two-shell model [21]. After a set of carefully designed experiments, Asami and Yonezawa [22] concluded that the cell wall, which is the outermost layer around the cell, can also contribute slightly to the high-frequency tail of the beta dielectric dispersion. The introduction of an additional layer into the model will carry with it two additional phase parameters — a conductivity and a permittivity term. Because in this paper we focus our attention to the dielectric constant of the plasma membrane, which contributes mostly to the low-frequency plateau (i.e., in the sub-MHz range) of the beta dispersion, the two-shell model constitutes an excellent approximation, while allowing us to keep the number of adjustable parameters to a minimum. The following paragraphs summarize the theory associated with the two-shell model, both for dilute and for concentrated suspensions of cells.

According to the Maxwell–Wagner mixture theory [23,24], the dielectric properties of a suspension of homogeneous spherical particles suspended in a medium with complex permittivity, $\varepsilon_a^* = \varepsilon_a + j\omega\kappa_a$ (with ε_a the true permittivity, k_a the conductivity, and $j=(-1)^{1/2}$), and subjected to an external alternating electrical field of angular frequency ω can be expressed as:

$$\varepsilon_s^* = \varepsilon_a^* \cdot \frac{(1+2\cdot\nu)\cdot\varepsilon_p^* + 2\cdot(1-\nu)\cdot\varepsilon_a^*}{(1-\nu)\cdot\varepsilon_p^* + (2+\nu)\cdot\varepsilon_a^*}. \quad (1)$$

Here $\varepsilon_s^* = \varepsilon_s + j\omega\kappa_s$ and $\varepsilon_p^* = \varepsilon_p + j\omega\kappa_p$ are the equivalent complex permittivity of the suspension of particles and of the

individual particles, respectively, while $v = \frac{\text{volume of cells}}{\text{volume of suspension}}$ is the volume fraction of the suspension. If the cells are covered by a thin, insulating membrane, ε_p^* presents frequency dependence and is given by:

$$\varepsilon_p^* = \varepsilon_{mc}^* \cdot \frac{(1+2\cdot v_{mc})\cdot \varepsilon_i^* + 2\cdot(1-v_{mc})\cdot \varepsilon_{mc}^*}{(1-v_{mc})\cdot \varepsilon_i^* + (2+v_{mc})\cdot \varepsilon_{mc}^*}, \quad (2)$$

where $v_{mc} = \left(1-\frac{d_{mc}}{R}\right)^3$.

The complex permittivity of the plasma membrane, which, as we shall see, is the parameter of main interest in this study, is represented by $\varepsilon_{mc}^* = \varepsilon_{mc} + j\omega\kappa_{mc}$. The parameter ε_i^* represents the complex permittivity of the interior region of the cells. Because the interior of the yeast cell contains membrane bound organelles, ε_i^* also depends on frequency. To account for the presence of (more or less concentric) organelles, such as the vacuole in the case of yeast, ε_i^* is written as:

$$\varepsilon_i^* = \varepsilon_{cp}^* \cdot \frac{(1+2\cdot v_o)\cdot \varepsilon_0^* + 2\cdot(1-v_o)\cdot \varepsilon_{cp}^*}{(1-v_o)\cdot \varepsilon_o^* + (2+v_o)\cdot \varepsilon_{cp}^*} \quad (3)$$

where $\varepsilon_{cp}^* = \varepsilon_{cp} + j\omega\kappa_{cp}$ represents the complex permittivity of the cytoplasm, and v_o, given by $\left[\frac{R_o}{R-d_{mc}}\right]^3$, stands for the fractional volume the organelle occupies inside the cell. Because the organelle is covered by a membrane (and is thereby inhomogeneous), ε_o^* is frequency dependent as expressed by:

$$\varepsilon_o^* = \varepsilon_{om}^* \cdot \frac{(1+2\cdot v_{om})\cdot \varepsilon_{io}^* + 2\cdot(1-v_{om})\cdot \varepsilon_{om}^*}{(1-v_{om})\cdot \varepsilon_{io}^* + (2+v_{om})\cdot \varepsilon_{om}^*}. \quad (4)$$

where $\varepsilon_{om}^* = \varepsilon_{om} + j\omega\kappa_{om}$ and $\varepsilon_{io}^* = \varepsilon_{io} + j\omega\kappa_{io}$ are the complex permittivity of the organelle membrane and interior of the organelle, respectively, and $v_{om} = \left(1-\frac{d_{om}}{R_o}\right)^3$.

For volume fractions of the particles higher than ~20%, the electric field sensed by a cell can no longer be considered homogeneous, due to the disturbances introduced by the other cells. Therefore, interactions between individual particles must be taken into account. Bruggeman [25], followed by Hanai [26,27], developed the effective medium theory (EMT), which achieves this goal; for volume fractions between 0.2 and 0.7 Bruggeman–Hanai theory has been confirmed to improve upon simulations obtained from Wagner's mixture equation [22,28,29]. Bruggeman–Hanai model starts from a dilute suspension of particles in which Eq. (1) describes the complex permittivity. Infinitesimal amounts of particles are added in small increments to the dilute suspension, resulting in a differential equation for the equivalent permittivity and volume fraction. The differential equation can be integrated numerically or, in some cases, analytically to provide the complex permittivity of the concentrated suspension of spherical cells [30,31]. The result of analytical integration is given by:

$$\left(\frac{\varepsilon_s^* - \varepsilon_p^*}{\varepsilon_a^* - \varepsilon_p^*}\right)\cdot\left(\frac{\varepsilon_a^*}{\varepsilon_s^*}\right)^{\frac{1}{3}} = 1 - v, \quad (5)$$

which provides means for estimation of the volume fraction (see Section 4), but it is rather difficult to solve for ε_s. Therefore, in this paper we used the numerical integration method described previously [30].

In the analysis presented in Section 4, we have tested both the Maxwell–Wagner, Eq. (1), and the Bruggeman–Hanai models (in its numerical form). The difference between the predictions of the two theories was small, due to the low cell volume fractions used; however, to avoid any ambiguity, we decided to use the Bruggeman–Hanai model.

3. Materials and methods

3.1. Sample preparation

Yeast cells (*S. cerevisiae*), engineered genetically to express a membrane receptor with a fluorescent tag attached to it, were prepared following a method described previously [11,32]. Briefly, one cell sample contained a plasmid, pYF2023, which contained a gene encoding the Sterile2-α factor receptor protein (Ste2p); this receptor is involved in cellular mating and is the protein of interest in this study. A gene encoding green fluorescent protein (GFP) – a widely used biologically compatible fluorescent tag which can be conveniently synthesized by the cell [33] – was fused inframe to the STE2 gene. Another plasmid (pYF2052), which contains all DNA from the first plasmid except those coding for STE2-GFP, was the control. Both types of cells were grown on plates containing synthetic medium lacking the vital amino acid uracil, which required the cells to maintain selection for the plasmid of interest (otherwise, the cells tend to loose the plasmid of interest). Plates were incubated at 30 °C for 2–3 days, and then small amounts were inoculated and cultured in yeast synthetic complete medium, containing 2% glucose and lacking uracil. The cultures were monitored by taking small batches periodically and testing for their optical absorption at 600 nm. After 12–20 h, the cells reached mid- to late-log phase and were harvested.

Approximately 32 ml of cell culture, with an optical density in the range of 1–3, were separated and centrifuged for 2 min at 5000 rpm. The supernatant was removed and the remaining pellet was initially suspended in 10 mM KCl for 45 min to wash out excess of electrolyte. Then, the cells were again separated from suspending medium by centrifugation, and resuspended in 20 mM KCl for 45 min. The cells were pelleted for a third time and suspended in 20 mM KCl. At this point the cells were well equilibrated with the KCl solution and ready for measurements.

All sample preparation procedures described above were performed at room temperature (~24 °C), unless otherwise specified.

3.2. Dielectric measurements

Equivalent parallel capacitance and conductance measurements of the yeast cell suspensions were carried out over a frequency range of 1 kHz–100 MHz (with 20 points per decade) using an Agilent 4294A precision impedance analyzer equipped

with a 16047E test clip fixture (Hewlett-Packard Company, Palo Alto, California) and a USB interface for computer control. The cell suspension was placed in a parallel plate capacitor (see Fig. 1) which was mounted in the test clip fixture for the whole duration of the experiment. Sample loading/unloading as well as rinsing of measuring cell with distilled water or KCl solution were done by using sterile syringes and an aspirator so as to avoid any changes in the lead inductances and capacitances that may occur due to mounting and unmounting the measuring cell.

At the beginning of each day of experiment, the measuring system was calibrated to compensate for inductance effects in the test leads by performing open/short measurements in accordance with the 16047E test fixture compensation procedure [34]. There is an electric field distribution outside of the sample chamber, leading to a capacitance in parallel with the admittance of the sample. To account for these fringe field effects, the two platinum electrodes are separated by a plexiglass spacer that extended radially past the platinum electrodes. The equivalent capacitance of the measuring cell (see Fig. 2) can be written as $C_m = C_o + C_s$, where C_m is measured capacitance, C_o is a stray capacitance (due to the field lines that close through the plastic spacer around the central hole that contains the sample), and C_s is cell suspension capacitance. The measured conductance, G_m (see Fig. 2), is the same as the suspension conductance, G_s, because the stray conductance is negligible due to the very low conductivity of the spacer material. The capacitance of a cylindrical suspension with electrodes capping the end of the cylinder is given by $C_s = \varepsilon_s \cdot \varepsilon_0 \cdot k$, where ε_s is the relative permittivity of the suspension, ε_0 ($=8.854 \times 10^{-12}$ F/m) is the permittivity of free space, and k is the geometrical cell constant [35] (which is approximately equal to the ratio between electrode surface area and the distance between the electrodes). The conductance of such a cylindrical suspension is given by $G_s = k \cdot \sigma_s$. The cell constant and the stray capacitance were calculated using measurements on samples with known electrical properties (distilled water and 20 mM KCl).

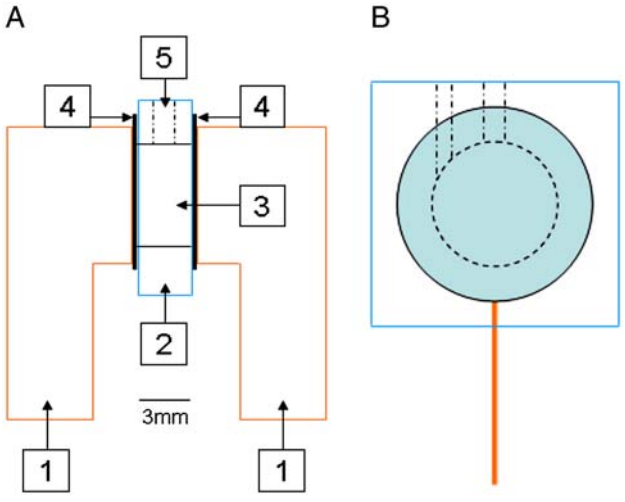

Fig. 1. Schematic of the measuring cell. (A) Main parts: 1 — copper leads; 2 — plexiglass spacer; 3 — sample chamber; 4 — platinized platinum disks; 5 — sample inlet. (B) Side view of the cell. The solid circle represents the area of the platinum disks (0.785 cm^2) and the dashed circle shows the size of the sample chamber (0.095 cm^3). The dashed lines represent pathways to sample chamber, one for filling the chamber with cell suspension, the other for removal of air.

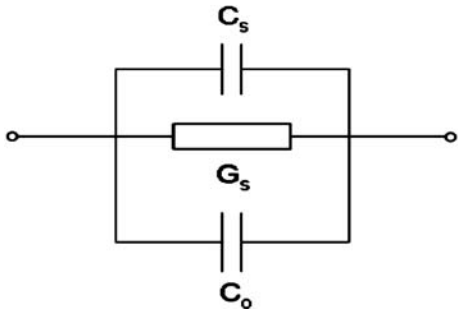

Fig. 2. Equivalent circuit of the cell after correction for inductance effects, where C_s and G_s are the capacitance and conductance of the sample, and C_o is the stray capacitance. Using measurements made on solutions with known dielectric properties, the stray capacitance was calculated and then subtracted from the measured capacitance, C_m, to obtain the capacitance of the suspension, C_s.

To reduce effects due to electrode polarization – an ubiquitous artifact in dielectric measurements in the audio/radiofrequency range –, the platinum electrodes were coated with a layer of platinum black using a method employed by Schwan [36]. This treatment increases the effective surface area of the electrodes, thereby reducing the polarization capacitance. Further corrections were performed for the remaining electrode polarization contributions as explained in Section 4. After dielectric measurements were performed on yeast cell samples, the suspension was immediately removed from the measuring cell and centrifuged. The equivalent capacitance and conductance of the supernatant were then determined by using the same procedure used for suspension.

3.3. Confocal laser scanning microscopy

Small amounts of sample were taken before starting dielectric measurements, and differential interference contrast (DIC) and fluorescence images of yeast cells were taken concomitantly with dielectric measurements by a different experimenter. A Leica™ confocal laser scanning microscope (Leica, IL) with an oil-immersion objective (magnification, 100× and NA = 1.3) was used to image the cells. The DIC images were used to determine the radii of the cells and vacuoles. Approximately 8 transmission images were taken for each sample, each containing several (~10) cells. The diameter of each cell was measured along two perpendicular directions, and the total volume of each spheroidal cell was calculated from these dimensions. The volume, averaged over all cells, was then used to determine the average cell radius. The cell radius used in the dielectric simulations was finally obtained by subtracting the cell wall thickness from the above radius. The value of the cell wall thickness (0.25 μm) was taken from the literature [37]. The same procedure was used to determine the average vacuole radius, except that no cell wall correction was necessary.

Fluorescence emission from GFP-tagged Ste2p was used to determine the presence of the Ste2p in the samples genetically engineered to overexpress the protein. The 476 nm line of an Argon-ion laser was used to excite the GFP fluorophore and the emission was separated by a dichroic mirror and recorded over a broad bandwidth (490–580 nm).

4. Results

Fig. 3 shows typical spectra for a cell suspension's relative permittivity and conductivity spectra of frequency. The sharp increase in permittivity and slight decrease in conductivity as the frequency decreases is due to electrode polarization (EP). This common artifact, observed at low-radio and audio frequency measurements, is due to the buildup of charge at the interface between electrode and electrolyte, which induces frequency-dependent contributions to the measured permittivity and conductivity. EP contribution overshadows the effect of the aforementioned alpha dispersion and any possible dielectric dispersions of the plasma membrane (see Discussion Section). In our experiments, it has been minimized by covering the platinum electrodes with a rough deposit of platinum black (see Section 3.2), but it cannot be removed completely. Electrode polarization has a long and interesting history. It has been usually modeled by dielectric spectroscopists with an equivalent circuit consisting of series combination of frequency-dependent capacitance, $C_p = A\omega^{-m}$, and resistance, $R_p = B\omega^{-n}$, connected in series with the sample [38]. This type of circuit has been used successfully to implement an EP correction method [39] appropriate for the case when the dielectric properties of the sample are constant at frequencies where frequency-dependent EP are observed (usually under ~1 MHz for physiological solutions). While this effectively takes into account the EP contributions to the measured permittivity and conductivity, it has been shown by Bordi et al. [40] that the four adjustable parameters (C_p and R_p) in the R–C series combination can be reduced to only two, if the following complex form is used for the following equivalent EP permittivity:

$$\varepsilon^*_{pol} = \left(i\varepsilon_o \frac{\omega}{f_e}\right)^{-m-1} \tag{6}$$

where m and f_e are two adjustable parameters. Eq. (6) is the well known constant-phase-angle law introduced by Jonscher [41] and it can be separated numerically, by using a computer, into a real and an imaginary part, corresponding to an equivalent parallel combination of permittivity and conductivity. The two EP components are thus related through the Kramers–Krönig relationship [19], which explains the collapse of the four adjustable parameters into only two. The graphs shown in Fig. 3 show the theoretical curves with and without the electrode polarization effect added to the model for the cell suspension (see Fig. 3 for details).

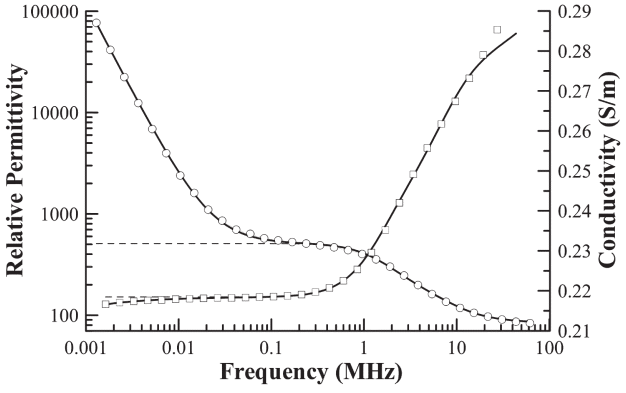

Fig. 3. Typical plots of relative permittivity (circles) and conductivity (squares) versus frequency for yeast cells expressing Ste2p (see text for details). The solid lines represent theoretical best fit predicted by the two-shell model described in the text, while the dashed lines correspond to the theoretical fit with the effect of electrode polarization subtracted off. Related parameters: d_{mc}=2.40 nm, d_{om}=2.40 nm, R=2.05 μm, R_0=1.16 μm, v=0.15, ε_{mc}=1.61, κ_{mc}=0 S/m, ε_a=78.1, κ_a=0.28 S/m, ε_{cp}=125, κ_{cp}=0.275 S/m, ε_{om}=2.36, κ_{om}=0 S/m, ε_{io}=60, κ_{io}=2.20 S/m, $f_e = 4.53\cdot10^{-5}$, m=0.755.

The experimental data were fitted to the two-shell model described in Section 2. There are several parameters that effect the dispersion curves in the β dispersion range, all of which cannot be determined from fittings of experimental data with the theoretical model. Therefore, independent experimental determinations provided three of these parameters, as follows. The average radius of the yeast cells was measured as described in Section 3.3. The outer medium conductivity and permittivity were determined by performing dielectric measurements on the supernatant resulting from centrifugation of the cell suspension. Once the outer medium conductivity was determined, the suspension's low-frequency conductivity together with the outer medium conductivity fixed the value of the volume fraction of the suspension, which is given in an approximate form by the equation [3]:

$$v = 1 - \left(\frac{\sigma_l}{\sigma_a}\right)^{\frac{2}{3}}. \tag{7}$$

Because the goal of this study has been to determine the extent to which membrane proteins are reflected in the permittivity of the plasma membrane, ε_{mc}, fixing three of the four major parameters in the fitting process leaves ε_{mc} as the only major fitting parameter to be determined. The permittivity and conductivity spectra of frequency were first fitted by visually comparing them to the theoretical model. Once the best visual fit was obtained, all the fitting parameters, excluding those that were pre-set according to the procedure described, were adjusted to minimize the fitting residual, given by:

$$\text{Residual} = \left[\frac{\sum_i \left(\log \varepsilon_{t,i} - \log \varepsilon_{d,i}\right)^2}{\sum_i \left(\log \varepsilon_{d,i}\right)^2} + \frac{\sum_i \left(\sigma_{t,i} - \sigma_{d,i}\right)^2}{\sum_i \left(\sigma_{d,i}\right)^2}\right]^{\frac{1}{2}} .100 \tag{8}$$

where the summation is over all frequencies (indexed by i), $\varepsilon_{t,i}$ and $\sigma_{t,i}$ are the theoretical suspension permittivity and conductivity for each frequency, and $\varepsilon_{d,i}$ and $\sigma_{d,i}$ are the experimental suspension permittivity and conductivity, respectively.

To confirm that the minimum value of the residual was the global minimum, the following process was employed: after a best fit between model predictions and experimental data was achieved, ε_{mc} was set to a value ~5% lower than what resulted from the global fit, and then a fitting was done by tuning all adjustable parameters except for ε_{mc}, so as to minimize the residual. Then, the value of ε_{mc} was increased by 0.5–1%, and the fitting process involving the other parameters was repeated. This process was repeated several times, and the minimum

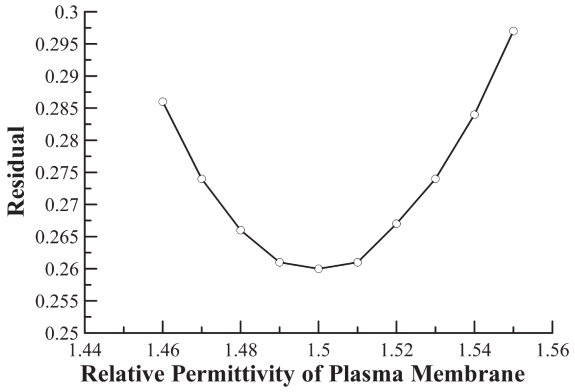

Fig. 4. Plot showing the fitting residual corresponding to best-fit values for the electrical phase parameters, for a typical suspension of cells expressing Ste2p receptors on their membrane. The parameter ε_{mc} was held fixed and all other parameters altered until the lowest residual was achieved. Each point in the plot represents the residual value plotted against the corresponding value for ε_{mc} used to achieve it. The minimum of the curve corresponds to the set of parameters that gives the overall best fit of the data.

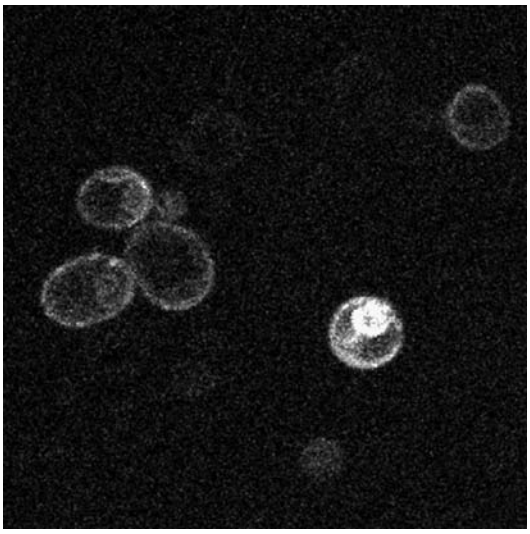

Fig. 5. Fluorescence image displaying visual evidence of yeast cells expressing Ste2 protein. Detection of light is done at 516 nm (±2.5 nm) for excitation with the 476-nm line of an Argon-ion laser.

values of the Residual corresponding to each fixed ε_{mc} value were recorded. A typical plot of the minimum residual values vs. ε_{mc} is shown in Fig. 4 for a suspension of cells expressing Ste2p receptors on their membrane. As can be seen, a distinct minimum occurs as a result of the process. The existence of the minimum in the plot clearly shows that the number of parameters used in data fitting in this paper is not larger than necessary. If that were not the case (i.e., if the number of adjustable parameters were too large) different values for, e.g., ε_{mc} would have led to the same value of the residual, which would indicate that the theoretical model is not appropriate for the cellular system used. It is therefore safe to choose the values of ε_{mc} for which the fitting residual reaches a minimum as most probable value of the membrane permittivity in the radio-frequency range.

The experiments described in Section 3 and the data analysis were repeated eight times for both types of cells, and the averages and standard deviations of the best-fit values for the electrical phase parameters corresponding to different cell compartments were calculated (see Table 1). Asami and Yonezawa [22] reported previously that the yeast cell wall contributes slightly to the β dispersion of the permittivity in the frequency range 10 to 100 MHz. We note that this contribution occurs far from the low-frequency plateau in permittivity, which we used to determine the values of ε_{mc}. This observation, together with the foreseen difficulties for the case when too many adjustable model parameters were included in the data analysis, determined us not to include the cell wall in the dielectric model of the cell. However, due to this simplification of the cell dielectric model, the values of those parameters contributing to the high frequency tail of the β dispersion (such as those corresponding to the interior of the vacuole, and even the permittivity of the vacuole membrane) were not analyzed and interpreted any further in this paper, because the cell wall might have contaminated their values.

Table 1
Average electrical phase parameters for wild type and control yeast cells plus or minus one standard deviation ($n=8$ experiments)

Sample	Relative membrane permittivity, ε_{mc}	Cytoplasm conductivity, κ_{cp} (S/m)	Relative vacuole membrane permittivity, ε_{om}
Ste2p-expressing	1.63±0.11	0.264±0.019	2.30±0.60
Wild type (no Ste2p)	1.75±0.16	0.307±0.041	2.25±0.55

The dominant parameter in the fitting process was the permittivity of the plasma membrane, ε_{mc}. The plasma membrane of eukaryotic cells has been extensively studied for years. At the beginning of our experiment, we hypothesized that in the cells expressing Ste2p, ε_{mc} would be significantly different from that of the control cells, because of the experimentally induced abundance of membrane proteins (see Fig. 5). Data in Table 1 indicate that this hypothesis is untenable. While the average values obtained for ε_{mc} do show a slight difference, it is not enough to overcome the spread in the data. A paired Student's t-test (two-tailed) returned a t value of 2.09, corresponding to a probability of 0.074 for the difference in the means to be statistically not significant (confidence level = 0.05). This is because the difference between the two values is within the standard deviation for each of the two sets, as seen in Table 1.

We therefore conclude that the permittivity of the plasma membrane in the radiofrequency range mainly reflects the properties of the phospholipids tails (see Section 5). Raicu and co-workers have speculated previously that plasma membrane permittivity in the radiofrequency range should only reflect the properties of the hydrophobic layer [21], but this paper provides the most direct evidence so far that addition of large numbers of proteins to the plasma membrane results in no noticeable changes in the dielectric constant of the membrane.

5. Discussion

Given the presence of high numbers of Ste2 proteins, in addition to other proteins normally present in the plasma membrane, one could legitimately ask the question, "why the presence of the proteins is not reflected in the value of ε_{mc}?" In this section, we attempt to answer this question and then suggest a few new possible directions of research that may eventually lead to the ability to detect the presence of receptor proteins on the plasma membrane, and, possibly their activity.

Previous studies on artificial as well as natural membranes have identified several structural regions of the plasma membrane, each characterized by different dielectric properties [42]. The regions include: a hydrophilic layer containing the polar heads of the phosphatidylcholine molecules making up the membrane, the hydrophobic region composed of the hydrocarbon chains of the molecules, and the region lying between these two labeled the acetyl region. Because of this configuration, the plasma membrane can be modeled as an electric circuit consisting of a series combination of parallel capacitances and conductances, each parallel combination corresponding to a layer of the membrane. This electrical circuit model, first proposed by Ashcroft et al. [43] is shown in Fig. 6. From this model, one can easily deduce that the equivalent capacitance and conductance of the membrane is frequency dependent, and presents three dispersion regions (i.e., $n-1=3$, corresponding to $n=4$ layers of the membrane, including the outer medium). Ashcroft et al. [7] showed that the interfacial polarization between the outer medium and the outermost layer of the membrane occurs at ~10 Hz [44]. Similarly, the interfacial polarization between subsequent layers occurs in the low-frequency regime, under 1000 Hz.

To be precise, Ashcroft et al [7] showed that more than four distinct layers can be actually inferred from dielectric measurements of pure phospholipid bilayers. This observation does not impact on our discussion in this paper, though it should have important implications for studies at lower frequencies than those used in this paper.

The Ste2 protein is an integral protein whose transmembrane domains span the membrane seven times [18]. The proteins might have a significant effect on the capacitance of the polar head region, but this effect isn't visible in the dielectric experiments that were carried out for this reason; the contribution to the equivalent capacitance of the membrane from the polar head regions is seen at low frequencies. Unfortunately, in the range of frequencies where the polar head region should contribute, the data are affected by the electrode polarization effect mentioned in Section 4. For higher frequencies, the capacitance of the membrane can be approximated by the equation [45]:

$$C \cong \frac{C_H}{1+\frac{2\cdot C_H}{C_P}},$$

in which C_H represents the capacitance of the hydrophobic layer. The acetyl and hydrophilic regions were pooled together to form an equivalent capacitance, C_P. The capacitance of the polar head region is generally two orders of magnitude larger than that of the hydrophobic region, therefore any significant change (e.g., 20%) in C_p brought by the presence of the proteins will only contribute a fraction of a percent to the equivalent capacitance of the membrane.

To observe any effect caused by the presence of the proteins in the beta dispersion range, attention must be turned to the hydrophobic portion of the plasma membrane, composed of a fluid-like matrix of lipids in which the hydrophobic portions of proteins are immersed. In this layer, the dielectric constant has been historically noted to depend strongly upon the hydrocarbon chains composing it [46]. The hydrophobic portion of the proteins present in this layer should alter the properties of these chains, but studies have shown that only the first few neighbors surrounding the proteins are affected. Marcelja [47] performed numeric simulations and estimated the disturbance caused by the presence of a nearby protein of an order parameter describing the orientations of hydrocarbon chains falls off rapidly after the first neighbor. Therefore, lipids, which largely contribute to the dielectric constant of the hydrophobic layer and thereby to ε_{mc}, are not altered enough to detect a change using linear dielectric spectroscopy.

Recent studies by Miller et al [14] using linear and nonlinear dielectric spectroscopy to study yeast cell cultures expressing the motor protein Prestin seem to confirm our observation above that little, if any, difference can be seen between the linear dielectric properties of suspensions of cells over-expressing and those not expressing the protein. Specifically, the Miller group developed a technique [48] that permits determination of the real and imaginary part of the complex permittivity at frequencies in the range of $10–10^5$ Hz. To quantify the difference between cells expressing Prestin and those not expressing it an index was defined as:

$$\Delta(f) = \frac{\varepsilon_p(f)}{\varepsilon_p(f_o)} - \frac{\varepsilon_c(f)}{\varepsilon_c(f_o)},$$

where the subscripts p and c stand for the Prestin yeast cell suspension and the control suspension, respectively. A plot of delta vs. frequency shows a peak around 25 kHz when f_o is equal to 10 kHz. The value given for $\Delta(f)$ at the peak frequency of 25 kHz was 0.5%, which seems to be even lower than our detected changes in plasma membrane permittivity. Slight variations in cell concentration could account for this small difference that might not be corrected for by the process of normalization described (because other contributions, such as electrode polarization might also be present). The permittivity

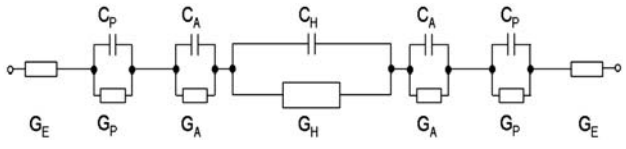

Fig. 6. Equivalent circuit describing the plasma membrane (according to Ashcroft, 1981). The series of parallel capacitances and conductances gives rise to a frequency dependent equivalent capacitance and conductance of the membrane. The subscripts used are as follows: "E" — surrounding electrolyte, "P" — polar head region, "A" — acetyl region, "H" — hydrophobic region.

measured at all frequencies depends on the volume fraction of the cells and on the conductivity of the suspending medium, which are susceptible to significant variability when using genetically engineered cells that overexpress proteins, such as those used in this work, since alterations in the cell metabolism are easily induced. It is precisely for this reason that in this work we took a different approach to data analysis. Our method, based on extraction of the relevant electrical parameters from the data, avoided the dependence of the results on parameters that bear no particular significance, while allowing us to determine the properties of the plasma membrane, where the proteins of interest in this work are located. Also, our method includes an analysis of the conductivity spectrum, which introduces further constraints to the possible values that the fitting parameters can take, increasing precision. Unfortunately, even after reducing such experimental errors, we were unable to detect significant alterations of the linear dielectric constant of the plasma membrane by the Ste2 proteins.

By contrast, we feel that the study using nonlinear dielectric spectroscopy performed by the same group is promising in its ability to detect the motor protein Prestin [14,49]. In the early 1990s, Woodward and Kell performed several studies [50–52] to show that systems perceived to be linear under an applied electric field can exhibit distinctive nonlinear properties, specifically the production of harmonics. In attempting to describe the ability of a system under linear conditions to demonstrate nonlinear capabilities, Woodward points to a description of the interesting features of protein interactions with electric fields as a potential source of these nonlinear occurrences. Miller and co-workers studied the generation of third harmonics from yeast cell suspensions with and without the ability to express Prestin, and found an astonishingly 40% difference between the two samples. If confirmed, this technique definitely promises to be an able method for detection of the presence of receptor proteins in the membrane and possibly their activity.

To return to the linear dielectric study described in this paper, we conclude that the permittivity of the plasma membrane in the radiofrequency range is dominated by the hydrophobic layer of the membrane, to which proteins might not make contributions large enough to be detectable. This observation in itself is important and may explain a previous finding that thermal treatment of the cells (which should induce protein denaturation), does not seem to affect the capacitance of the plasma membrane [53]. We believe that, if further research could lead to methods for reduction or even elimination of the electrode polarization contribution to the dielectric properties of cell suspension, it may become possible to probe the presence of proteins in the plasma membrane from linear dielectric studies.

References

[1] H. Fricke, S. Morse, The electric resistance and capacity of blood for frequencies between 800 and 4.5 Million cycles, J. Gen. Physiol. 9 (1925) 153–167.

[2] H. Fricke, The electric capacity of suspensions with special reference to blood, J. Gen. Physiol. 9 (1925) 137–152.

[3] K. Asami, T. Yamaguchi, Dielectric spectroscopy of plant protoplasts, Biophys. J. 63 (1992) 1493–1499.

[4] A. Irimajiri, M. Ando, R. Matsuoka, T. Ichinowatari, S. Takeuchi, Dielectric monitoring of rouleaux formation in human whole blood: a feasibility study, Biochim. Biophys. Acta 1290 (1996) 207–209.

[5] K. Asami, E. Gheorghiu, T. Yonezawa, Real-time monitoring of yeast cell division by dielectric spectroscopy, Biophys. J. 76 (1999) 3345–3348.

[6] V. Raicu, T. Saibara, A. Irimajiri, Multifrequency method for dielectric monitoring of cold-preserved organs, Phys. Med. Biol. 45 (2000) 1397–1407.

[7] H.G.L. Coster, T.C. Chilcott, A.C.F. Coster, Impedance spectroscopy of interfaces, membranes and ultrastructures, Bioelectrochem. Bioenerg. 40 (1996) 79–98.

[8] J. Lippincott-Schwartz, G.H. Patterson, Development and use of fluorescent protein markers in living cells, Science 300 (2003) 87–91.

[9] D.J. Stephens, V.J. Allan, Light microscopy techniques for live cell imaging, Science 300 (2003) 82–86.

[10] M. Yang, G. Luiken, E. Baranov, R.M. Hoffman, Facile whole-body imaging of internal fluorescent tumors in mice with an LED flashlight, BioTechniques 39 (2005) 170–172.

[11] V. Raicu, D.B. Jansma, R.J. Miller, J.D. Friesen, Protein interaction quantified in vivo by spectrally resolved fluorescence resonance energy transfer, Biochem. J. 385 (2005) 265–277.

[12] R.M. Clegg, Fluorescence resonance energy transfer, in: X.F. Wang, B. Herman (Eds.), Fluorescence Imaging Spectroscopy and Microscopy, Wiley-Interscience, New York, 1996.

[13] J.R. Lakowicz, Principles of Fluorescence Spectroscopy, Kluwer Academic/Plenum Publishers, New York, 1999.

[14] J. H Miller, D. Nawarathna, D. Warmflash, F.A. Pereira, W.E. Brownell, Dielectric properties of yeast cells expressed with the motor protein prestin, J. Biol. Phys. 31 (2005) 465–475.

[15] G.J. Ciambrone, V.F. Liu, D.C. Lin, R.P. McGuinness, G.K. Leung, S. Pitchford, Cellular dielectric spectroscopy: a powerful new approach to label-free cellular analysis, J. Biomol. Screen. 9 (2004) 467–480.

[16] W.K. Kroeze, D.J. Sheffler, B.L. Roth, G-protein-coupled receptors at a glance, J. Cell Sci. 116 (2003) 4867–4869.

[17] K.J. Blumer, J.E. Reneke, J. Thorner, The STE2 gene product is the ligand-binding component of the alpha-factor receptor of *Saccharomyces cerevisiae*, J. Biol. Chem. 263 (1988) 10836–10842.

[18] M.C. Overton, S.L. Chinault, K.J. Blumer, Oligomerization of G-protein-coupled receptors: lessons from the yeast *Saccharomyces cerevisiae*, Eukaryot. Cell 4 (2005) 1963–1970.

[19] K.R. Foster, H.P. Schwan, Dielectric properties of tissues, in: C. Polk, E. Postow (Eds.), Handbook of Biological Effects of Electromagnetic Fields, CRC Press, Boca Raton, 1996, pp. 25–102.

[20] A. Irimajiri, T. Hanai, A. Inouye, A dielectric theory of multi-stratified shell model with its application to a lymphoma cell, J. Theor. Biol. 78 (1979) 251–269.

[21] V. Raicu, G. Raicu, G. Turcu, Dielectric properties of yeast cells as simulated by the two-shell model, Biochim. Biophys. Acta, Bioenerg. 1274 (1996) 143–148.

[22] K. Asami, T. Yonezawa, Dielectric behavior of wild-type yeast and vacuole-deficient mutant over a frequency range of 10 kHz to 10 GHz, Biophys. J. 71 (1996) 2192–2200.

[23] J.C. Maxwell, A Treatise on Electricity and Magnetism, Clarendon Press, Oxford, 1891.

[24] K.W. Wagner, Arch. Elektrotech. 2 (1914) 371–387.

[25] D.A.G. Bruggeman, Berechnug vershiedener physikalischen Konstanten von heterogenen Substanzen, Ann. Phys. (Leipz.) 24 (1935) 636–664.

[26] T. Hanai, Theory of the dielectric dispersion due to the interfacial polarization and its application to emulsion, Kolloid-Z. 171 (1960) 23–31.

[27] T. Hanai, Electrical properties of emulsions, in: P. Sherman (Ed.), Emulsion Science, Academic Press, New York, 1968, pp. 353–478.

[28] A. Irimajiri, T. Hanai, A. Inouye, Evaluation of a conductometric method to determine the volume fraction of the suspensions of biomembrane-bounded particles, Experientia 31 (1975) 1373–1375.

[29] M. Clausse, Dielectric properties of emulsions and related systems, in: P. Becher (Ed.), Encyclopedia of Emulsion Technology, Marcel Dekker Inc., New York, 1983, pp. 481–715.

[30] V. Raicu, T. Saibara, H. Enzan, A. Irimajiri, Dielectric properties of rat liver in vivo: analysis by modeling hepatocytes in the tissue architecture, Bioelectrochem. Bioenerg. 47 (1998) 333–342.
[31] K. Asami, Characterization of heterogeneous systems by dielectric spectroscopy, Prog. Colloid & Polym. Sci. 27 (2002) 1617–1659.
[32] M.C. Overton, K.J. Blumer, Use of fluorescence resonance energy transfer to analyze oligomerization of G-protein-coupled receptors expressed in yeast, Methods 27 (2002) 324–332.
[33] R.Y. Tsien, The green fluorescent protein, Annu. Rev. Biochem. 67 (1998) 509–544.
[34] Hewlett-Packard, Hewlett-Packard User Manual.
[35] H.P. Schwan, Electrical properties of tissue and cell suspensions, in: J.H. Lawrence, C.A. Tobias (Eds.), Advances in Biological and Medical Physics, Academic Press, New York, 1957, pp. 147–209.
[36] H.P. Schwan, Determination of biological impedances, in: W.L. Nastuk (Ed.), Physical Techniques in Biological Research, Academic Press, New York, 1963, pp. 323–407.
[37] E. Vitols, R.J. North, A.W. Linnane, Studies on the oxidative metabolism of *Saccharomyces cerevisiae*. I. Observations on the fine structure of the yeast cell, J. Biophys. Biochem. Cytol. 9 (1961) 689–699.
[38] H.P. Schwan, Electrode polarization impedance and measurements in biological materials, Ann. N.Y. Acad. Sci. 148 (1968) 191–209.
[39] V. Raicu, T. Saibara, A. Irimajiri, Dielectric properties of rat liver in vivo: a noninvasive approach using an open-ended coaxial probe at audio/radio frequencies, Bioelectrochem. Bioenerg. 47 (1998) 325–332.
[40] F. Bordi, C. Cametti, R.H. Colby, Dielectric spectroscopy and conductivity of polyelectrolyte solutions, J. Phys., Condens. Matter 16 (2004) R1423–R1463.
[41] A.K. Jonscher, Universal Relaxation Law, Chelsea Dielectrics, London, 1996.
[42] H.G. Coster, J.R. Smith, The molecular organisation of bimolecular lipid membranes. A study of the low frequency Maxwell–Wagner impedance dispersion, Biochim. Biophys. Acta 373 (1974) 151–164.
[43] R.G. Ashcroft, H.G. Coster, J.R. Smith, The molecular organisation of bimolecular lipid membranes. The dielectric structure of the hydrophilic/hydrophobic interface, Biochim. Biophys. Acta 643 (1981) 191–204.
[44] R.G. Ashcroft, H.G. Coster, J.R. Smith, The molecular organisation of bimolecular lipid membranes. The effect of benzyl alcohol on the structure, Biochim. Biophys. Acta 469 (1977) 13–22.
[45] D.R. Laver, J.R. Smith, H.G.L. Coster, The thickness of the hydrophobic and polar regions of glycerol monooleate bilayers determined from the frequency-dependence of bilayer capacitance, Biochim. Biophys. Acta 772 (1984) 1–9.
[46] R. Fettiplace, D.M. Andrews, D.A. Haydon, The thickness, composition, and structure of some lipid bilayers and natural membranes, J. Membr. Biol. 5 (1971) 277–296.
[47] S. Marcelja, Lipid-mediated protein interaction in membranes, Biochim. Biophys. Acta 455 (1976) 1–7.
[48] C. Prodan, F. Mayo, J.R. Claycomb, J.H. Miller, M.J. Benedik, Low-frequency, low-field dielectric spectroscopy of living cell suspensions, J. Appl. Phys. 95 (2004) 3754–3756.
[49] D. Nawarathna, J.R. Claycomb, G. Cardenas, J. Gardner, D. Warmflash, J.H. Miller, W.R. Widger, Harmonic generation by yeast cells in response to low-frequency electric fields, Phys. Rev., E Stat. Phys. Plasmas Fluids Relat. Interdiscip. Topics 73 (2006) 051914.
[50] A.M. Woodward, D.B. Kell, On the nonlinear dielectric-properties of biological-systems *Saccharomyces cerevisiae*, Bioelectrochem. Bioenerg. 24 (1990) 83–100.
[51] A.M. Woodward, D.B. Kell, On the relationship between the nonlinear dielectric-properties and respiratory activity of the obligately aerobic bacterium *Micrococcus luteus*, Bioelectrochem. Bioenerg. 26 (1991) 423–439.
[52] A.M. Woodward, D.B. Kell, Dual-frequency excitation — a novel method for probing the nonlinear dielectric-properties of biological-systems, and its application to suspensions of *Saccharomyces cerevisiae*, Bioelectrochem. Bioenerg. 25 (1991) 395–413.
[53] Y. Huang, R. Holzel, R. Pethig, X.B. Wang, Differences in the AC electrodynamics of viable and non-viable yeast cells determined through combined dielectrophoresis and electrorotation studies, Phys. Med. Biol. 37 (1992) 1499–1517.